Yb(III), Sm(III) and La(III) complexes of a tetradentate pyridoxal Schiff base ligand: their DNA-binding activity and bio-imaging applications

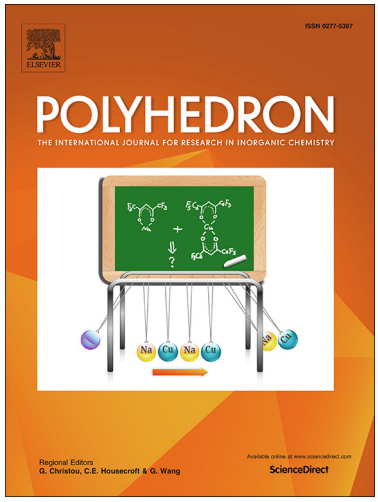

Yb(III), Sm(III) and La(III) complexes of a tetradentate pyridoxal Schiff base ligand: their DNA-binding activity and bio-imaging applications

Moumita Chakraborty, Satyajit Mondal, Christine Cardin, Arnold L. Rheingold, Chitrangada Das Mukhopadhyay, Shyamal Kumar Chattopadhyay

PII: S0277-5387(19)30604-7
DOI: https://doi.org/10.1016/j.poly.2019.114167
Reference: POLY 114167

To appear in: *Polyhedron*

Received Date: 15 July 2019
Accepted Date: 3 October 2019

Please cite this article as: M. Chakraborty, S. Mondal, C. Cardin, A.L. Rheingold, C. Das Mukhopadhyay, S. Kumar Chattopadhyay, Yb(III), Sm(III) and La(III) complexes of a tetradentate pyridoxal Schiff base ligand: their DNA-binding activity and bio-imaging applications, *Polyhedron* (2019), doi: https://doi.org/10.1016/j.poly.2019.114167

Yb(III), Sm(III) and La(III) complexes of a tetradentate pyridoxal Schiff base ligand: their DNA-binding activity and bio-imaging applications

Moumita Chakraborty,[a] Satyajit Mondal,[a] Christine Cardin,[b] Arnold L. Rheingold,[c] Chitrangada Das Mukhopadhyay,[d] Shyamal Kumar Chattopadhyay[a,*]

[a]Department of Chemistry, Indian Institute of Engineering Science and Technology, Shibpur, Howrah 711 103, India, Fax: +91 033 2668 2916; e-mail: shch20@hotmail.com

[b]Department of Chemistry, The University of Reading, Whiteknights, Reading, Berkshire, RG6 6AH United Kingdom.

[c]Department of Chemistry, University of California, San Diego, Urey Hall 5128, La Jolla, CA 92093-0358, USA.

[d]Centre for Healthcare Science and Technology, Indian Institute of Engineering Science and Technology, Shibpur, Howrah 711 103, India.

ABSTRACT

Yb(III), Sm(III) and La(III) complexes of a tetradentate Schiff base ligand, bis(pyridoxylidene)ethyelenediamine, are reported. Single crystal X-ray crystal structures of the complexes reveal that in all of them the Ln(III) ions are in a distorted dodecahedral geometry with N_4O_4-coordination environment provided by two coordinated ligands. Fluorescence spectroscopy shows that in the Yb(III) and Sm(III) complexes energy transfer from ligand centered excited state leads to population of emissive f-f excited states. The reported complexes bind to ct-DNA, with high binding constant (K_b) comparable to those which bind by intercalative mode. Cytotoxicity study shows that the complexes have quite low cytotoxicity towards HeLa cell. Further, they exhibited fast response, bright fluorescence and stability at physiological pH, making them suitable for use in fluorescence bio-imaging.

Keywords: Yb(III), Sm(III), La(IIII), DNA-binding, Cytotoxicity, fluorescence bio-imaging

1. Introduction

Schiff bases, condensation products of aldehydes or ketones and amines, play an important role in co-ordination chemistry, forming complexes of varied oxidation states with wide range of metal ions [1]. Schiff base metal complexes also play potent roles in, biological modelling of metalloenzymes [2-4], synthesis of molecular ferromagnets [5,6] and liquid crystals [7,8], catalysis [9,10], medical imaging [11] and as synthons for crystal engineering [12-17].

Pyridoxal, a vitamer of vitamin B6, is the most versatile co-factor in biological systems [18-20]. It participates in a plethora of important biological reactions e.g. transamination, deamination, decarboxylation, which are vital for amino acid metabolism, besides being a key player in synthesis of important neurotransmitter like GABA and serotonin [21-30]. Therefore, interest in exploration of metal complexes with pyridoxal type ligands is justified as they are highly biocompatible. The fluorescence properties of pyridoxal offer the additional possibility of using pyridoxal appended ligands as fluorescent probes, sensors and imaging agents [31, 32]. Reasonably good aqueous solubility of pyridoxal Schiff base ligands and complexes are an aid to their possible biological applications.

Metal complexes with strong DNA binding affinity are of increasing importance due to their possible applications in medicinal research. They are potential DNA molecular probes and chemotherapeutic reagents [33-35]. Metal complexes bind to DNA via three major modes: intercalation, groove binding and electrostatic interactions [36-38].

Lanthanides, referring to the elements from La to Lu are progressively emerging as promising luminescent probes for biology and medicine [39, 40]. Lanthanides and their complexes are not only used as sensors for biologically relevant species like DNA but also serve as DNA cleaving agents [41]. Lanthanide complexes have poor steriochemical preferences and high co-ordination number and thus can be suitable designed to achieve efficient DNA cleavage activity and cytotoxicity [42]. There are also interesting reports of dual functional water soluble Gd(III) and Yb(III) complexes in literature, which can be used for imaging as well as photodyanamic therapy [43,44]. Moreover, lanthanides act as enzyme inhibitors [45, 46] as they are hard Lewis acids. In spite of such properties, reports on DNA binding study of lanthanide complexes are relatively few in literature.

2. Experimental section

2.1. Physical Methods and Materials

Pyridoxal hydrochloride, ethylenediamine, $Sm(NO_3)_3{\cdot}6H_2O$, $Yb(NO_3)_3{\cdot}6H_2O$ and $La(NO_3)_3{\cdot}6H_2O$ were obtained from either Aldrich or E. Merck or CDH. Calf-thymus DNA (ct-DNA) was from GeNei. All other chemicals, synthesis grade and spectroscopic grade solvents were obtained from Merck, Aldrich or Spectrochem. Elemental analyses were performed on a Perkin Elmer 2400 carbon, hydrogen, and nitrogen analyzer. UV−Vis spectra were recorded using a JASCO V-530 spectrophotometer. Electron spray ionization mass spectrometry (ESI-MS) spectra of the samples were recorded on a JEOL JMS 600 instrument. Fluorescence spectra and TCSPC experiments were carried out using Horiba Instruments made Fluorolog-3 modular spectrofluorometer using a Xe arc lamp (for recording spectra) or a 330 nm Pulsed LED light source for TCSPC experiments. The absolute quantum yield for the ligand centered transition of the complexes (**1-3**) in DMF solution were calculated by using the F3029 integrating sphere accessory, the Quanta-φ. This includes recording excitation source intensity and calculating the area under the corrected emission spectra. Further the relative quantum yield of the metal centered transition for complex **2** was calculated using the formula given below taking the ligand centered transition of the same complex as standard.

$$\frac{\Phi}{\Phi_r} = \frac{OD_r}{OD} \cdot \frac{\eta^2}{\eta_r^2} \cdot \frac{A}{A_r}$$

2.2. Synthesis of ligand

The dihydrochloride ligand was prepared as described in our earlier work [47]. For synthesis of the complexes the neutral ligand was prepared *in situ* by reacting an methanolic solution of pyridoxal hydrochloride, whose pH was adjusted to 6-7 with concentrated aqueous KOH, and ethylenediamine dissolved in minimum volume in methanol.

2.3. Syntheses of Ln(III) Complexes 1-3

The complexes **1**, **2** and **3** were synthesized using a general procedure. Detailed synthetic method for complex **1** is given below as a representative example.

2.3.1. Synthesis of $Yb(LH_2)_2(NO_3)_2Cl{\cdot}H_2O$ (1)

To a methanolic solution of the neutral ligand LH_2 (0.36g, 1mmol) prepared *in situ* $Yb(NO_3)_3{\cdot}6H_2O$ (0.233g, 0.5mmol) was added and the solution was stirred for 4 hrs. The pale yellow solid was filtered, washed with diethylether and dried over fused calcium chloride. Yield: 83%. Anal. Calc. for $C_{36}H_{46}N_{10}O_{15}ClYb$: C 40.55; H 4.22; N 13.13; Found: C 40.75; H 4.32; N 13.09. MS: m/z:

888.50[Yb(LH)$_2$]$^+$ (100%)], (Fig: S1 in the ESI†). Electronic spectrum in DMF solution: λ_{max}/nm (ε_{max}/M^{-1} cm^{-1}): 355(18570), 941(2.40), 978(2.78).

2.3.2. Synthesis of Sm(LH$_2$)$_2$(NO$_3$)$_3$·3H$_2$O (2)

Yield: 85%. Anal. Calc. for $C_{36}H_{50}N_{11}O_{20}Sm$: C 39.04; H 4.51; N 13.90; Found: C 39.12; H 4.49; N 13.82. MS: m/z: 866.43[Sm(LH)$_2$]$^+$ (100%)], (Fig: S2 in the ESI†). Electronic spectrum (DMF solution) λ_{max}/nm (ε_{max}/M^{-1} cm^{-1}): 360(10572), 955(23.66), 1080(22.05).

2.3.3. Synthesis of La(L)(LH)·3H$_2$O(3)

Yield: 89%. Anal. Calc. for $C_{36}H_{47}N_8O_{11}La$: C 47.68; H 5.84; N 12.35; Found: C 47.56; H5.80; N 12.23. MS: m/z: 853.38 [LaL$_2$]$^+$ (100%)], (Fig: S3 in the ESI†). Electronic spectrum (DMF solution) λ_{max}/nm (ε_{max}/M^{-1} cm^{-1}): 365(10764).

2.4. X-ray crystallography

Single crystal X-ray data were collected for **1** and **2** on a Bruker SMART APEX-II CCD area diffractometer at 100 (2) and 293(2)K respectively using Mo-Kα radiation (0.71073 Å). Absorption corrections were employed using SADABS [48], data solution was achieved by direct methods and refined by full matrix least squares on F^2 using SHELXL version 2014/7 for **1** and SHELXL-97 for **2** [49]**.** The non-hydrogen atoms were refined with anisotropic displacement parameters. All hydrogen atoms were placed at calculated positions and refined as riding atoms for **1** and mixed model for **2**, using isotropic displacement parameters. For **3** the data were collected on an Oxford Gemini diffractometer at 150 K using Cu-Kα radiation (1.54180 Å). Data were corrected for absorption effects using CrysAlis program [50] and solved by direct methods by full matrix least squares on F^2 using CRYSTALS [51]. The H atoms were located in a difference map, but H-atoms bonded to carbon were placed in their geometric positions. The H atoms were initially refined isotropically with soft restraints on the bond lengths and angles to regularize their geometry. One of the H-atom attached to C25 carbon atom in complex **1** could not be located due to disorder.
A summary of the crystallographic data is given in Table 1. Important metrical parameters are collected in Tables 2 and S1. Crystallographic CCDC numbers are 1903592-1903594 for **1**-**3** respectively.

2.5. DNA-binding experiments

2.5.1 Absorption spectroscopic studies

Concentration of ct-DNA was determined using absorbance at 260 nm with molar extinction co-efficient (ε) = 6600 M^{-1} cm^{-1} [52]. The details experimental procedure is same as that described by us earlier [53]. To the 1×10^{-5} M solution of complex increments of the ct-DNA solutions [1×10^{-4} M] were added. The complex-DNA solutions were homogenised for 5 min before the absorption spectra were recorded. The stability of the complexes in aqueous Tris-HCl buffer (pH 7.4) medium was ascertained by checking the lifetime of the complexes for a time interval of 0-7h by TCSPC experiments.

2.5.2 Fluorescence binding study

To perform fluorescence quenching experiments, equimolar mixture of classical intercalator ethidium bromide (EB) /ct–DNA (DNA concentration 5x10^{-6} M) was prepared in Tris-HCl (pH 7.4) buffer solution by pre-treating ct-DNA with EB and storing the solution at 4°C for 4 h, to which increments of a 1×10^{-5} M stock solution of Ln(III) complexes were added and emission intensities were measured using a Horiba made model Fluorolog-3 modular multifunctional TCSPC lifetime spectrofluorometer. The solutions were excited at 520 nm and the emissions were recorded in the range of 540 and 700 nm.

2.6. Cytotoxicity Study

Confocal Imaging Study of Cells and MTT Cell Viability Assay are performed following the experimental procedure reported in our previous publication [54].

3. Result and discussion

3.1. Synthesis of complexes

The ligand bis(pyridoxylidene)ethylenediamine(LH_2) was obtained as dihydrochloride salt by the action of methanolic solution of ethylenediamine (1eqv.) on methanolic solution of pyridoxal hydrochloride (2eqv.). The Ln(III) complexes were obtained by reacting the *in situ* prepared neutral ligand with a methanolic solution of the Yb(III), Sm(III) and La(III) nitrate salt in a 2:1 molar proportion in MeOH medium at room temperature (Scheme 1) when the complex separates out from the reaction mediums in very good yields(80-90%). The Yb(III) and the Sm(III) complexes crystallized as tripositive cations having all the four pyridine nitrogen atoms belonging to two tetradentate ligands being protonated. The La(III) complex on the other hand is a neutral complex, having one dinegative and another mono negative ligand with one of the pyridine nitrogens being protonated. for the later. To prove the point we have done conductivity measurement in DMF medium at 298K.

Molar conductance of **1**, **2** and **3** were calculated as 189 Ω^{-1} cm^2 M^{-1}, 252 Ω^{-1} cm^2 M^{-1} and 42 Ω^{-1} cm^2 M^{-1} which suggests that **1** and **2** are 1:3 electrolyte whereas **3** is an non-electrolyte [55]. The relatively small size of Yb(III) and Sm(III) ions compared to La(III) probably results in higher acidity of solutions of the salts of the former two ions, which results in protonation of the pyridine nitrogens in their complexes during synthesis. However, as shown below, the Uv-Vis and fluorescence spectra of the complexes in Tris-HCl buffer (pH 7.4) suggest that in the buffer solutions all the complexes have same state of protonation. The elemental analyses and the ESI-MS spectra of **1**, **2** and **3** are in agreement to their formulation as bis(pyridoxylidene)ethylenediamine complexes of Yb(III), Sm(III) and La(III). The ESI-MS data were collected in dilute aqueous solution of the complexes which indicate that our complexes are fairly stable in aqueous medium.

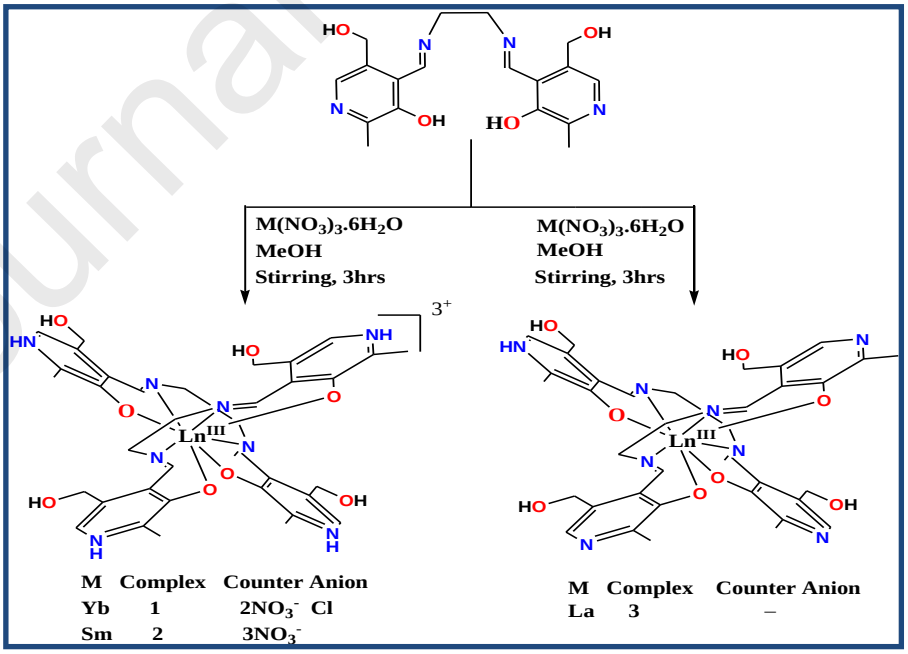

Scheme1. Schematic depiction of the synthesis of Ln(III) complexes.

3.2. Electronic Spectroscopy

3.2.1. Absorption Spectra

The electronic absorption spectra of the ligand and their complexes (**1**-**3**) were reported in the range of 250–1100 nm in DMF medium (Figure 1a). The electronic spectrum of the free ligand shows a broad intense band at 335nm which in the complexes are marginally shifted to longer wavelengths (355nm for **1**; 360nm for **2**; 365nm for **3**). This peak can be attributed to the phenolate O pπ→imine π*. The relatively larger red shift for the La(III) complex (complex **3**) may be attributed to the different degree of protonation of this complex compared to the Yb(III) and Sm(III) complexes (complexes **1** and **2**). This is supported by the fact that in tris-HCl buffer (pH =7.4) the band appears almost at the same position (at around 360 nm) for all the complexes. A broad peak centred around 430nm in the free ligand is assigned n→π* transition and this band is absent in the complexes. For the Sm(III) complex two transitions at 955 nm and 1080 nm are assigned to f-f transitions ($^6H_{5/2} \rightarrow {}^6F_{11/2}$, $^6F_{9/2}$) (Figure S8) [56, 57]. For the Yb(III) complex the f-f transition ($^2F_{7/2} \rightarrow {}^2F_{5/2}$) is observed as a doublet at 941 nm and 978 nm, due to Stark splitting (Figure 1b).

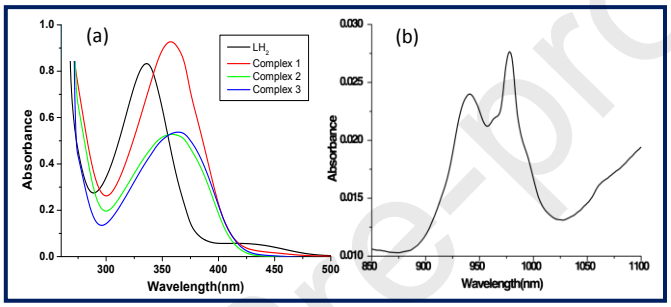

Fig. 1. Electronic absorption spectra of ligand and complexes (**1**-**3**) in DMF at UV-Vis region (a) and f-f band of Complex **1** in NIR region (b).

3.2.2. Emission spectra

The fluorescence emission spectra of the free ligand and the Ln(III) complexes were measured in DMF solutions (Figure 2). The free ligand shows emission at 383 nm, when excited at 335 nm, and this may be assigned to emission from the pyridoxal chromophore. The lifetime of the excited state was estimated to be 2.82×10^{-9}s from the TCSPC experiments (Figure S9). In the La(III) complex (**3**), the emission is observed at 462 nm and the excited state lifetime was found to be 6.46×10^{-8}s (Table 1). Evidently, on complexation with the La(III) ion the excited state is considerably red shifted and its lifetime increased by approximately 23-fold. For the Yb(III) and Sm(III) complexes (**1** and **2**) there is only a small red shift (of 20 nm) of the ligand centered emission and its lifetime is decreased by an order of magnitude with the values being 1.80×10^{-10}s, 2.97×10^{-10}s for **1** and **2** respectively. This decrease of the lifetime of the ligand centred excited state in **1** and **2** is due to sensitization of f-f excited state in these complexes by energy transfer process. Again, the relatively large red-shift of the ligand centred emission in DMF solution of the La(III) complex compared to Yb(III) and Sm(III) complexes may be ascribed to the different degree of protonation of the ligands in the La(III) complex compared to other two complexes. When the spectra were recorded in Tris-HCl buffer (pH 7.4) the emission maxima of all the three complexes are observed at nearly the same position (Figure S10).

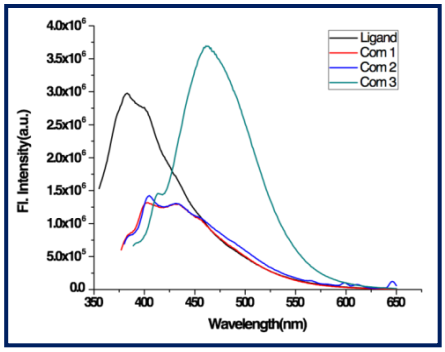

Fig. 2. Emission spectra of ligand (λ_{ext}=335nm) and complexes (λ_{ext}=355nm, 360nm, 365nm for complexes **1**, **2** and **3** respectively) in DMF [1×10^{-5} M].

At room temperature, besides the ligand centered (LC) emission, **1** and **2** also show metal centred (MC, f-f) emissions (Figure 3). The emission spectrum of **1** shows a doublet at 992nm and 1024nm, which is due to Stark splitting of $^2F_{5/2} \rightarrow {}^2F_{7/2}$ transition [58,59]. For complex **2**, the metal centred emissions are observed in the 550-700 nm region. The dominant emission peak is at 646 nm corresponding to the $^4G_{5/2} \rightarrow {}^6H_{9/2}$ transition, while two other emission peaks at 566 and 598 nm are due to the $^4G_{5/2} \rightarrow {}^6H_{5/2}$ and $^4G_{5/2} \rightarrow {}^6H_{7/2}$ transitions, the latter two peaks showing doublet structure due to stark splitting in asymmetric ligand environment [59]. The quantum yield of the MC emission for complex **2** was estimated as 0.0131 (Table 1) with reference to the quantum yield of the LC emission of the same complex. However, quantum yield of the MC emission of the corresponding Yb(III) complex could not be evaluated in the same way as the detectors for LC and MC emissions were different.

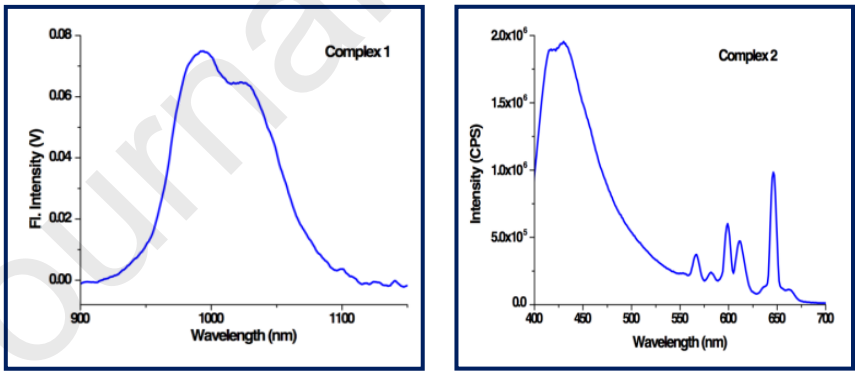

Fig. 3. Metal-centred emission spectra of complexes **1** and **2** at room temperature in DMF.

Table 1

Emission spectral characteristics of the complexes in DMF solutions

Complex	Quantum yield of the Ligand centered emission and their lifetimes	Metal Centered Transition
1	0.0181, 1.80×10^{-10}s	-
2	0.0362, 2.97×10^{-10}s	0.0131
3	0.0513, 6.46×10^{-8}s	-

3.3. Description of the X-ray crystal structures

The ORTEP diagrams of **1**, **2** and **3** are given in Figure 4. Crystal data and refinement details of **1**, **2** and **3** are given in Table 2 and selected bond distances are given in Table 3 while selected bond angles are given in Table S1. Of the three complexes reported here, complex **1** crystallizes with one water molecule of crystallization, while complexes **2** and **3** crystallize with three water molecules of crystallization.

The octa-coordinated lanthanide centres in all the three complexes adopt distorted dodecahedral geometries with LnN_4O_4 chromophores, the metal atom coordinates to four phenolic O atoms and four imine N atoms of the two tetradentate Schiff base ligands.

The bond lengths in all the complexes are unexceptional, albeit at the lower side of the range generally found for complexes of these metal ions with N_4O_4-donor environment [59-63]. Expectedly, for a given metal ion M–O distances are considerably shorter than the M–N distances. Also both M–O and M–N distances are shortest in the Yb(III) complex and longest in the La(III) complex with the Sm(III) complex having the values in between.

Table 2

Crystal data and refinement details of complexes **1**, **2** and **3**.

Compound	**1**	**2**	**3**
Formula	$C_{36}H_{45}N_{10}O_{15}ClYb$	$C_{36}H_{50}N_{11}O_{20}Sm$	$C_{36}H_{47}N_8O_{11}La$
Formula Weight	1066.31	1107.23	906.72
Crystal Size	0.34x0.3x0.24	0.26x0.24x0.22	0.034x0.07x0.082
T(K)	100(2)	293(2)	150(2)
Crystal system	Monoclinic	Monoclinic	Monoclinic

Space Group	P $2_1/c$	P $2_1/n$	P $2_1/n$
a(Å)	11.9805(8)	11.7413(6)	10.48135(18)
b(Å)	14.9324(9)	31.0905(15)	29.1130(4)
c(Å)	22.7945(13)	12.0463(6)	13.4065(3)
α(°)	90	90	90
β(°)	101.808(2)	98.4140(10)	101.1778(18)
γ(°)	90	90	90
D_{calc}(g cm^{-3})	1.774	1.691	1.501
μ(mm^{-1})	2.496	1.445	8.800
F(000)	2152	2260.0	1856
Total reflections	25658	40845	6050
Unique reflections	8105	7660	6016
Observed data[I>2σ(I)]	6399	7226	4801
R_{int}	0.0322	0.0273	0.054
R_1, wR_2 [I>2σ(I)]	0.0399,0961	0.0275,0.0637	0.0437,0.1141
R_1, wR_2 (all data)	0.0561,0.1064	0.0298,0.0647	0.0605,0.1255
Goodness-of-fit (GOF) on F^2	1.039	1.195	1.0122

Table 3

Selected bond distances(Å) of complexes **1**, **2** and **3**.

Bond distances (Å)					
1		**2**		**3**	
Yb1-O1	2.244(3)	Sm1-O1	2.3040(19)	La1-O2	2.420(4)
Yb1-O4	2.216(3)	Sm1-O2	2.3171(18)	La1-O17	2.405(4)
Yb1-O5	2.252(3)	Sm1-O6	2.2945(18)	La1-O28	2.415(4)
Yb1-O8	2.227(3)	Sm1-O7	2.3637(18)	La1-O46	2.385(4)
Yb1-N2	2.456(4)	Sm1-N1	2.584(2)	La1-N10	2.693(4)
Yb1-N3	2.476(4)	Sm1-N2	2.571(2)	La1-N13	2.659(4)
Yb1-N6	2.469(4)	Sm1-N5	2.568(2)	La1-N39	2.657(4)
Yb1-N7	2.480(4)	Sm1-N6	2.563(2)	La1-N42	2.677(4)

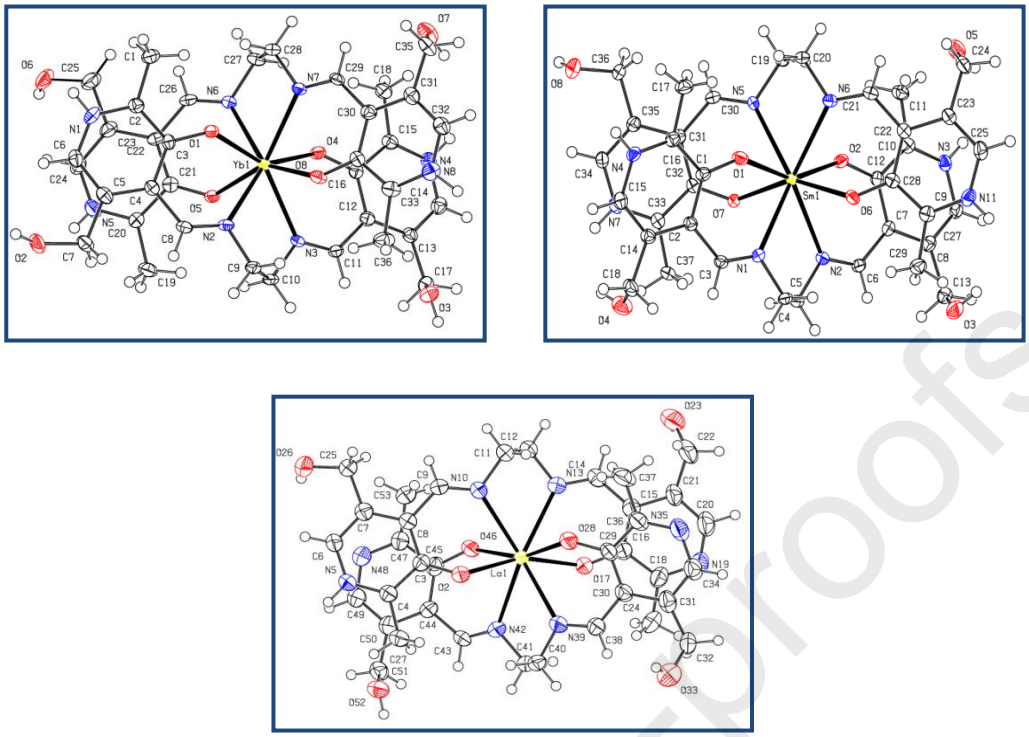

Fig. 4. ORTEP diagram (50% probability ellipsoids) of the complex unit of **1**(top left), **2**(top right) and **3**(bottom).

2.4. DNA binding study

2.4.1. Absorption Spectroscopic Study

In order to investigate the binding modes of metal complexes with DNA we have considered electronic absorption spectroscopic technique. A complex generally exhibits hypochromism and a red shift (bathochromism) of its absorption band when it intercalate to DNA, causing a strong stacking interaction amongst the adjacent base pairs of DNA and the aromatic chromophore of the complex. The extent of the hypochromism commonly parallels the intercalative binding strength. To establish the binding affinity of the complexes to ct-DNA, the change in absorption intensities of complexes (**1-3**) were recorded at a constant concentration (1×10^{-5}M) with increments of CT-DNA in aqueous medium (10^{-2} M of Tris–HCl buffer, pH 7.4) (Figure 5 and Figure S11). The addition of ct-DNA induced a pronounced hypochromicity with no red shift in wavelength. The intrinsic binding constant (K_b) for the interaction of the Ln(III) complexes with ct-DNA was calculated using the following equation :

$$[DNA]/\varepsilon_a-\varepsilon_f = [DNA]/\varepsilon_b-\varepsilon_f + 1/K_b(\varepsilon_b-\varepsilon_f) \qquad (1)$$

In this equation the term ε_a refers to the extinction coefficient observed (A_{obs}/M), ε_b and ε_f are the extinction coefficient of the compound when fully bound to DNA and the extinction coefficient of the free compound respectively. From the straight line plot of $[DNA]/(\varepsilon_a-\varepsilon_f)$ vs.[DNA], K_b was determined as the ratio of the slope to intercept.

The binding of **1** with DNA leads to a decrease in the absorption intensity at 316 nm, with a slight increase in intensity at 252 nm, whereas for **2** and **3,** along with a decrease in intensity at 316nm band, a new band appears at 252nm. All three complexes show an isosbestic point (at 292nm for **1**, at 294nm for **2** and at 291nm for **3**). The DNA binding constant (K_b) value using absorptions at 316nm was calculated to be 9.04×10^5 M^{-1}, 2.76×10^5 M^{-1} and 2.16×10^5 M^{-1} for **1**, **2** and **3** respectively. The TCSPC experiments reveal

that the average lifetime of the complexes (Table S2) in aqueous Tris-Hcl buffer (pH 7.4) medium for a range of 0-7h remains almost unaltered indicating the stability of the complexes during the DNA-binding experiments.

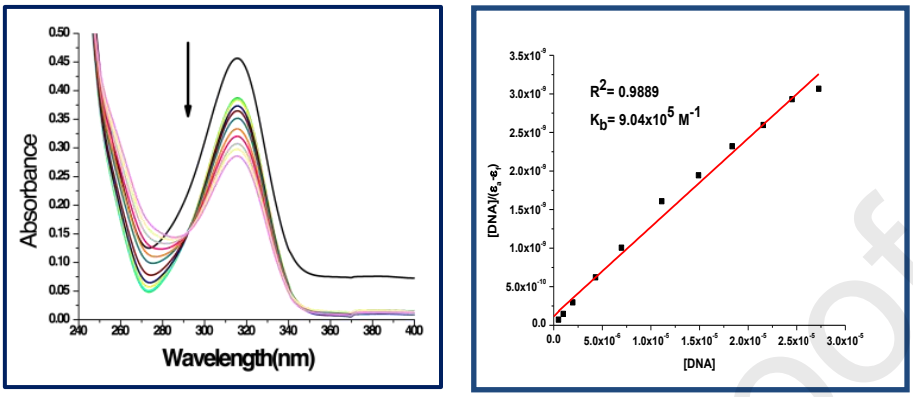

Fig. 5. Absorption spectra of **1** in the absence and presence of increasing amount of CT-DNA at 25 ºC in 0.01M aqueous Tris–HCl buffer (pH 7.4) and the respective plot of [DNA]/(ε_a-ε_f) vs. [DNA].

3.4.2. Fluorescence Spectroscopic Study

Fluorescence spectral study is a potent method employed to study the binding of the complexes to ct-DNA using ethidium bromide as a fluorescent probe. EB in buffer medium shows low emission intensity which gets significantly enhanced when intercalated into the base pairs of DNA. Further binding of the complex to DNA would lead to quenching of the emission intensity as the complex displaces the bound EB from the ct-DNA-EB system.The emission spectra of ct-DNA-EB system in the absence and presence of **1**, **2** and **3** are shown in Figure 6 and Figure S12. The above quenching data can be analyzed by calculating the quenching constant (K_{sv}) based on Stern-Volmer equation $I_0/I=1+K_{sv}[Q]$; I and I_0 are the fluorescence intensities in the presence and absence of the quencher (**1**, **2** and **3**) respectively. K_{sv} is the Stern-Volmer quenching constant and [Q] is the quencher concentration. The quenching data are in agreement with the Stern-Volmer equation with K_{sv} values 1.54×10^5 M^{-1}, 1.83×10^5 M^{-1}, 1.64×10^5 M^{-1} for **1**, **2** and **3** respectively. The apparent binding constant (K_{app}) value is calculated from the equation :

$$K_{app}\times [complex]_{50} = K_{Eb}\times [EB]$$

where Kapp is the apparent binding constant of the complex, [complex] is the complex concentration at 50% reduction of fluorescence intensity of EB-DNA system, K_{EB} is the binding constant of ethidium bromide (K_{EB}= $1.0\times10^7 M^{-1}$)[52], and [EB] is the concentration of ethidium bromide(10μM). The K_{app} values calculated are 1.05×10^7 M^{-1}, 1.16×10^7 M^{-1} and 1.14×10^7 M^{-1} for **1**, **2** and **3** respectively. It appears that the K_{app} values are two orders of magnitude higher than the K_b values found for these complexes in earlier section, using Uv-Vis spectroscopy. This apparent discrepancy is due to the use of the K_{EB} value (K_{EB}= $1.0\times10^7 M^{-1}$) from the literature [52]. We have earlier reported the K_{EB} value of 1×10^5 M^{-1} for the calf-thymus DNA used by us in our experimental conditions [53]. Using this K_{EB} value we get K_{app} values of 1.05×10^5 M^{-1}, 1.16×10^5 M^{-1} and 1.14×10^5 M^{-1} for complexes **1**, **2** and **3** respectively, which is in good agreement with their K_b values. As mentioned earlier during discussion of absorption and emission spectra of the complexes, in the Tris-HCl buffer, used in this work, all the complexes appear to exist in the same state of protonation of the ligands and therefore the similarity of their DNA-binding constants are justified in spite of their apparently different charges in the solid state or DMF solutions.

As all the three complexes are sufficiently fluorescent we have also studied the quenching of the fluorescence of the complex solution in presence of increasing amounts of ct-DNA. The emission spectra of

the complexes in the absence and presence of ct-DNA are shown in Figure 7 and Figures S13 and S14. The above quenching data were also evaluated based on the Stern-Volmer equation, $I_0/I = 1 + k_{SV}[Q]$; where I and I_0 are the fluorescence intensities in the presence and absence of the quencher (ct-DNA) respectively, Ksv is the Stern Volmer quenching constant and [Q] is the quencher concentration. The Ksv values for **1**, **2** and **3** were calculated as 4.76×10^5 M^{-1}, 0.87×10^5 M^{-1} and 2.24×10^5 M^{-1} respectively.

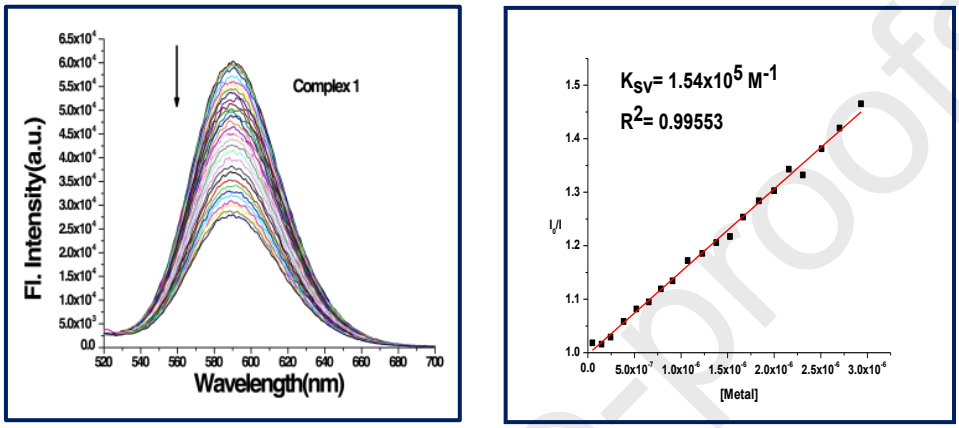

Fig. 6. Emission spectra of EB bound DNA with increasing amounts of **1** (left) and the corresponding Stern- Volmer plot (right).

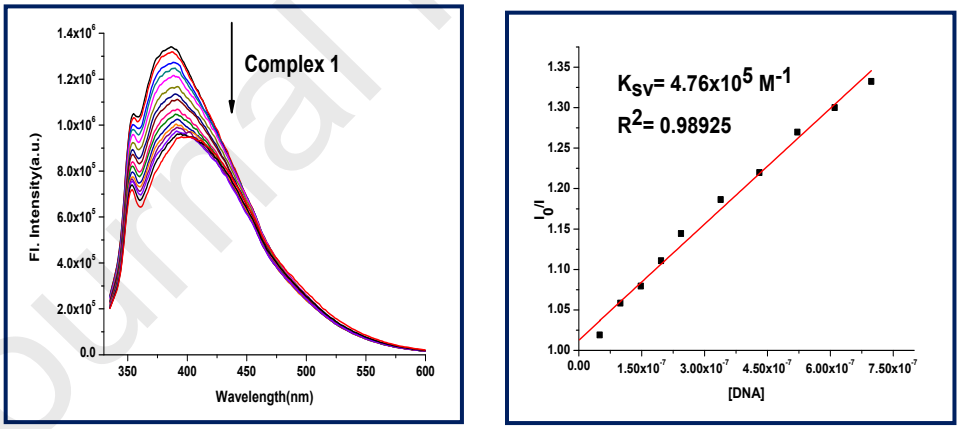

Fig. 7. Emission spectra of **1** with increasing amounts of ct-DNA solution at 315nm (left) with their respective I_0/I vs. [DNA] plot (right).

3.5. Cytotoxicity Study

MTT assay showed that the cytotoxicity was dose dependent with increasing concentration of the complexes. CC50 values for the **1** (Yb 1), **2** (Sm 1) and **3** (La 1) were found to be 280µM, 200µm and

260μm concentrations (Figure 8 and Figure S15). The low cytotoxicity of the complexes along with their bright fluorescence, fast response and stability at physiological pH make them suitable candidates for cellular imaging studies. The fluorescence images were recorded before and after the addition of the complex (20 μM) (Figure 9 and Figure S16). The complexes can penetrate the cells with ease making no morphometric distortions in case of HeLa cells. Cells incubated in absence of the probe exhibited no fluorescence, whereas a bright fluorescence signal was detected in the cells stained with complexes (1-3). Thus from this cytotoxicity study we can infer the cell membrane permeability of the complexes and hence they can be effectively employed as biological imaging probe.

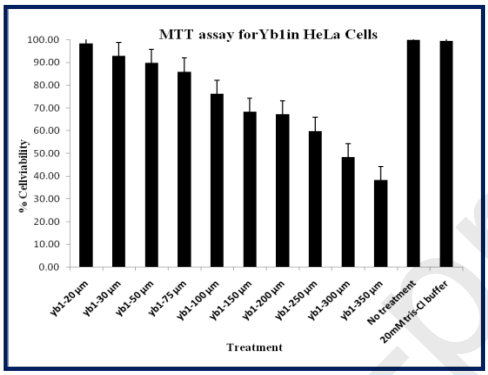

Fig. 8. Cytotoxicity study of **1** on HeLa cells.

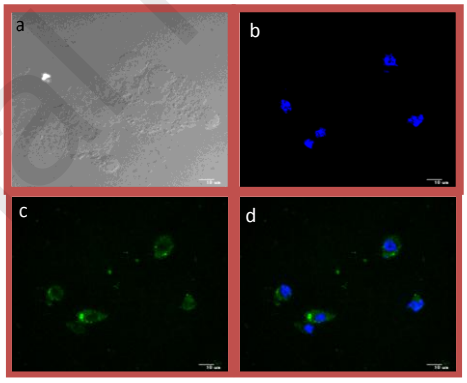

Fig. 9. Confocal microscopic images (images obtained with 100 X objective lens) of HeLa cells (a) Bright field image of cells (b) fluorescence images of cells in absence of probe (**1**), nuclei counterstained with Hoechst 33342 fluorescent stain (1 mg/mL) (c) fluorescence images of cells in presence of probe (**1**), excited at 405 nm (d) image of (b) and (c) overlaid.

4. Conclusions

Pyridoxal being one of the most versatile co-factor in biological systems their Schiff base complexes are very attractive subjects for investigation. These complexes are potential DNA molecular probes and chemotherapeutic reagents. With this point of view we have described three water soluble complexes of Yb(III), Sm(III) and La(III) containing a tetradentate ligand bearing two pyridoxal moieties. The Yb(III)

and Sm(III) complexes show ligand sensitized f-f emission, the emission of the Yb(III) complex falling in the NIR region which makes it potential candidate for possible applications in optical communications and fluoroimmunoassay. The complexes show strong DNA binding ability against calf thymus DNA. We have also shown that the three lanthanide complexes have low toxicity and they can be used for cellular imaging.

Acknowledgements

MC gratefully acknowledge IIEST, Shibpur for awarding her Institute Fellowship. SKC thanks DST, West Bengal, for providing partial funding of this work.

References

[1] R.H. Holm, J. Am. Chem. Soc. 82 (1960) 5632-5636.

[2] E.C. Niederhoffer, J.H. Timmons, J.H. Timmons, A.E. Martell, Chem. Rev. 84 (1984) 137-203.

[3] C.O. Rodriguez de Barbarin, N.A. Bailey, D.E. Fenton, Q.-Yu. He, J. Chem. Soc.,Dalton Trans. (1997) 161-166.

[4] E.J. Larson, V.L. Pecoraro, J. Am. Chem. Soc. 113 (1991) 3810-3818.

[5] J.-M. Lehn, Supramolecular Chemistry, VCH, Weinheim (1995) p113.

[6] R.E.P. Winpenny, Chem. Soc. Rev. 27 (1998) 447-452 .

[7] R.W. Date, E.F. Iglesias, K.E. Rowe, J.M. Elliott, D.W. Bruce, Dalton Trans. (2003) 1914-1931.

[8] E. Terazzi, S. Torelli, G. Bernardinelli, J.-P. Rivera, J.-M. Bénech, C. Bourgogne, B.Donnio, D. Guillon, D. Imbert, J.-C.G. Bünzli, A. Pinto, D. Jeannerat, C. Piguet, J.Am. Chem. Soc. 127 (2005**)** 888-903.

[9] E. Tsuchida, K. Oyaizu, Coord. Chem. Rev. 237 (2003**)** 213-228.

[10] L. Canali, D.C. Sherrington, Chem. Soc. Rev. 28 (1999) 85-93.

[11] F. Tisato, F. Refosco, F. Bandoli, Coord. Chem. Rev. 135 **(**1994) 325.

[12] S. Naskar, D. Mishra, S.K. Chattopadhyay, M. Corbella, A.J. Blake, Dalton Trans. 53 **(**2005) 2428-2435.

[13] S. Naskar, D. Mishra, R.J. Butcher, S.K. Chattopadhyay, Polyhedron 26 (2007) 3703-3714.

[14] M. Prabhakar, P.S. Zacharias, S.K. Das, Inorg. Chem. 44 (2005) 2585-2587.

[15] Z. He, C. He, E.-Q. Gao, Z.-M. Wang, X.-F. Yang, C.-S. Liao, C.-H. Yan, Inorg. Chem. 42 (2003) 2206-2208.

[16] S. Naskar, M. Corbella, A.J. Blake, S.K. Chattopadhyay, Dalton Trans. (2007) 1150-1159.

[17]S. Naskar, S. Naskar, R. J. Butcher, S. K. Chattopadhyay, Inorg. Chim. Acta 363 (2010**)** 404-411.

[18] V. Snitsarev, T. Budde, T. P. Stricker, J. M. Cox, D. J. Krupa, L. Geng, A. R. Kay, Biophys. J. 80 (2001) 1538-1546.

[19] Y. Mikata, M. Wakamatsu, A. Kawamura, N. Yamanaka, S. Yano, A. Odani, K. Morihiro, S. Tamotsu, Inorg. Chem. 45 **(**2006) 9262-9268.

[20] Y. Mikata, M. Wakamatsu, S. Yano, Dalton Trans. 3 (2005**)** 545-550.

[21] W. Gan, S. B. Jones, J. H. Reibenspies, R. D. Hancock, Inorg. Chim. Acta 358 **(**2005) 3958-3966.

[22] C. Bazzicalupi, A. Bencini, A. Bianchi, C. Giorgi, V. Fusi, B. Valtancoli, M. A. Bernado, F. Pina, Inorg. Chem. 38 (1999**)** 3806-3813.

[23] C. Bazzicalupi, A. Bencini, E. Berni, A. Bianchi, P. Fornasari, C. Giorgi, B. Valtancoli, Eur. J. Inorg. Chem. 10 (2003) 1974-1983.

[24] E. Kimura, T. Koike, Chem. Soc. Rev. **(**1998**)** 27 179-184.

[25] L. Stryer, Biochemistry, 4th Ed. **(**1995) p631.

[26] S. Dakshinamurti, K. Dakshinamurti, in: J. Zempleni, R. B. Rucker, D. B. MaCormick, J. W. Suttie (Eds.), Handbook of Vitamins, CRC Press, Boca Raton, FL, USA (2007) 315.

[27] J. Casas, M. D. Couce, J. Sordo, Coord. Chem. Rev. (2012) 256 3036-3062.

[28] A.D. Mackey, S.R. Davis, J.F. Gregory III, in: M.E. Shils, M. Shike, A.C. Ross, B. Caballero, R.J. Cousins (Eds.), Modern Nutrition in Health and Disease, Xth ed., Lippincott Williams & Wilkins, Philadelphia, USA (2006) 452-461.

[29] S. Sharif, D. Schagen, M.D. Toney, H.-H. Limbach, J. Am. Chem. Soc. 129 (2007) 4440-4455.

[30] P. Christen, D. E. Metzler, Transaminases, 1st ed. Wiley: New York, **(**1985) pp 37.

[31]C. Das, B. Pakhira, A. L. Rheingold, S. K. Chattopadhyay, Inorg. Chim. Acta 482 (2018) 292-298.

[32]S. Mondal, P. Adak, C. Das, S. Naskar, B. Pakhira, A. L. Rheingold, E. Sinn, C. S. Eribal, S. K. Chattopadhyay, Polyhedron 81 (2014) 428-435.

[33] V. Rajendiran, R. Karthik, M. Palaniandavar, H. Stoeckli-Evans, V. S. Periasamy, M. A. Akbarsha, B. S. Srinag, H. Krishnamurthy, Inorg. Chem. 46 (2007) 8208-8221.

[34] P. T. Selvi, H. Stoeckli-Evans, M. Palaniandavar, J. Inorg. Biochem. 99 (2005) 2110-2118.

[35]E. R. Jamieson, S. J. Lippard, Chem. Rev. 99 (1999) 2467-2498.

[36] H. L. Wu, J. K. Yuan, Y. Bai, G. L. Pan, H. Wang, J. Kong, X. Y. Fan, H. M. Liu, Dalton Trans. 41 (2012) 8829-8838.

[37] H. L. Wu, J. K. Yuan, Y. Bai, G. L. Pan, H. Wang, X. B. Shu, J. Photoch. Photobiol. B. 107 (2012) 65-72.

[38] P. Kumar, B. Baidya, S. K. Chaturvedi, R. H. Khan, D. Manna, Inorg. Chim. Acta 376 (2011) 264-270.

[39] S. Kobayashi, M. Sugiura, H. Kitagawa and W. W. L. Lam, Chem. Rev. 102 (2002) 2227-2302.

[40] F. Wang, Y. Han, C. S. Lim, Y. H. Lu, J. Wang, J. Xu, H. Y. Chen, C. Zhang, M. H. Hong and X. G. Liu, Nature 463 (2010) 1061-1065.

[41] M. Komiyama, Y. Aiba, Y. Yamamoto and J. Sumaoka, Nat. Protoc. 3(2008) 655-662.

[42] A. Hussain, S. Gadadhar, T. K. Goswami, A. A. Karande, A. R. Chakravarty, Dalton Trans. 41 (2012) 885-895.

[43] T. Zhang, R. Lan, C. –F. Chan, G. –L. Law, W. -K. Wong, K. –L. Wong, Proc. Natl. Acad. Sci. USA, 111 (2014), E5492-E5497.

[44] J. -X Zhang, H. Li, C. –F. Chan, R. Lan, W. –L. Chan, G. –L. Law, W. –K. Wong, K. –L. Wong, Chem. Commun. 48 (2012) 9646–9648

[45] L. Feig, M. Panek, W. D. Horrocks Jr and O. C. Uhlenbech, Chem. Biol. 6 (1999) 801-810.

[46]H. –K. Kim, J. Li, N. Nagraj and Y. Lu, Chem. –Eur. J. 14 (2008) 8696-8703.

[47]S. Naskar, S. Naskar, R. J. Butcher, S. K. Chattopadhyay, Inorg. Chim. Acta 363 (2010) 404-411.

[48] SADABS (version 2.03); Bruker AXS Inc., Madison, WI (2002).

[49] G. M. Sheldrick, Acta Crystallogr. Sect. A64 (2008) 112-122.

[50]CrysAlisPro: Oxford Diffraction (2010).

[51] P. W. Betteridge, J. R. Carruthers, R. I. Cooper, K. Prout, D. J. Watkin, J. Appl. Cryst. 36 (2003) 1487.

[52] M. E. Reichmann, S. A. Rice, C. A. Thomas, P.Doty, J. Am. Chem. Soc. 76 (1954**)** 3047-3053.

[53] S. Mondal, B. Pakhira, A. J. Blake, M. G. B. Drew, S. K. Chattopadhyay, Polyhedron 117 (2016**)** 327-337.

[54] P. Adak, B. Ghosh, A. Bauz´a, A. Frontera, A. J. Blake, M. Corbella, C. Das Mukhopadhyay, S. K. Chattopadhyay, RSC Adv. 6 (2016) 86851-86861

[55]W.J. Geary, Coord. Chem. Rev. (1971) 81-122.

[56]Y.A. Tanko, M.R. Sahar, S.K. Ghoshal, Results in Physics 6 (2016) 7-11.

[57]Y. –X. Chi, S. Y. Niu, J. Jin, R. Wang, Y. Li, Dalton Trans. 47 (2009) 7653-7659.

[58]K. T. Hua, J. Xu, E. E. Quiroz, S. Lopez, A. J. Ingram, V. A. Johnson, A. R. Tisch, A. de Bettencourt-Dias, D. A. Straus, G. Muller, Inorg. Chem. 51 (2012) 647-660.

[59] A. N. Gusev, V. F. Shul'gin, S. B. Meshkova, M. Hasegawa, G. G. Alexandrov, I. L. Eremenko, W. Linert, Polyhedron 47 (2012**)** 37-45.

[60]L. Pavelek , V. Ladányi, M. Necˇas, Z. Moravec , K. Wichterle, Polyhedron 119 (2016) 134-141.

[61] W. Xie, M. J. Heeg, P. G. Wang, Inorg. Chem. 38 (1999) 2541-2543.

[62]Z. –F. Chen, Y. –Q. Gu, X. –Y. Song, Y. –C. Liu, Y. Peng, H. Liang, Eur. J. Med. Chem 59 (2013) 194-202.

[63] G. –J. Chen, Z. –G. Wang, X. Qiao, J. –Y. Xu, J. –l. Tian, S. –P. Yan, J. Inorg. Biochem. 127 (2013) 39-45.

Graphical Abstract

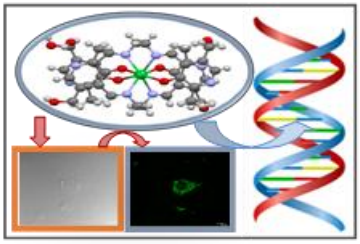

Yb(III), Sm(III) and La(III) complexes of a tetradentate Schiff base ligand, bis(pyridoxylidene) ethyelenediamine are reported. The complexes bind ct-DNA very strongly by intercalation mode. The low toxicity and bright fluorescence of the complexes can be used for bio-imaging.

Supporting Information

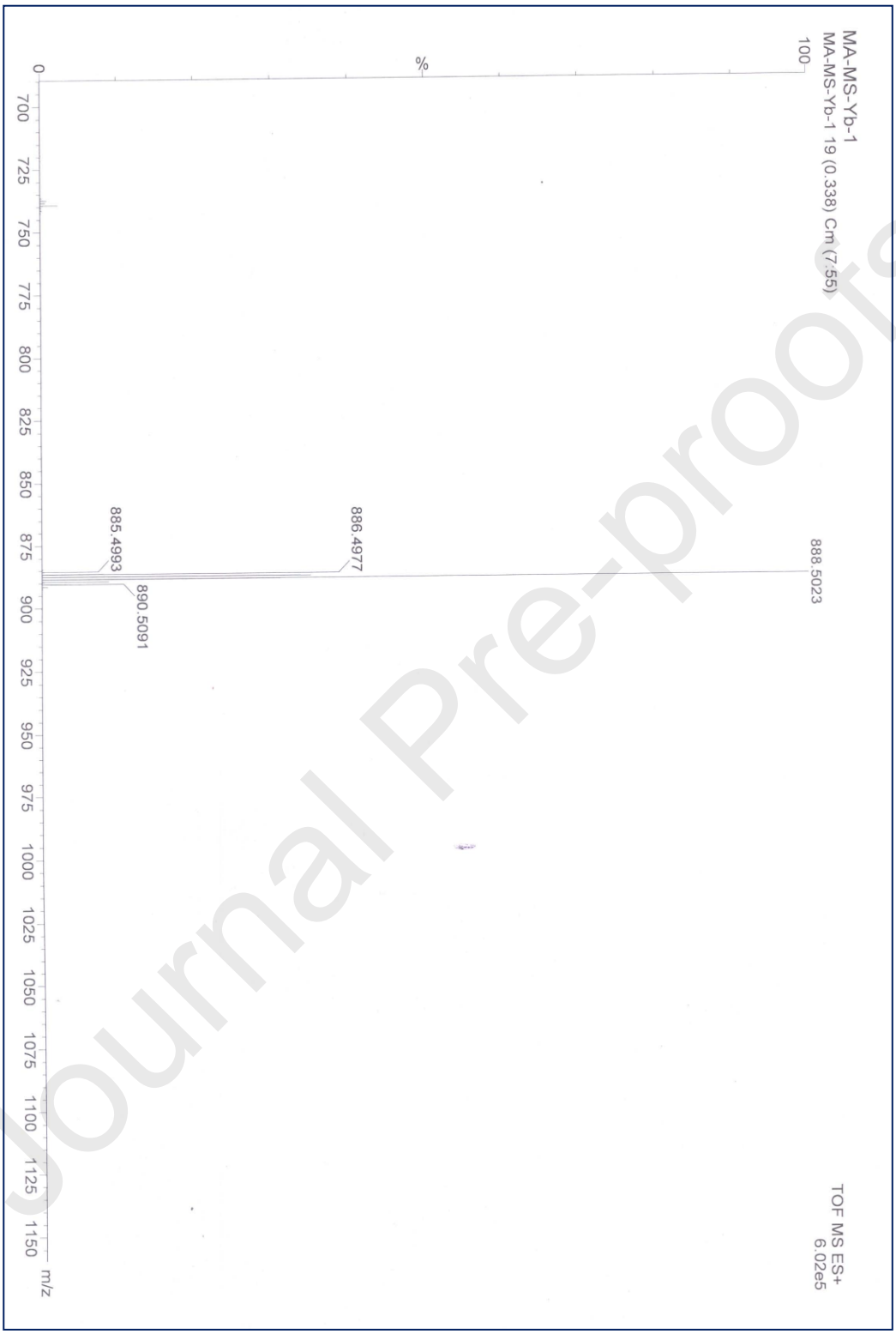

Figure S1. ESI-MS Spectra of **1**.

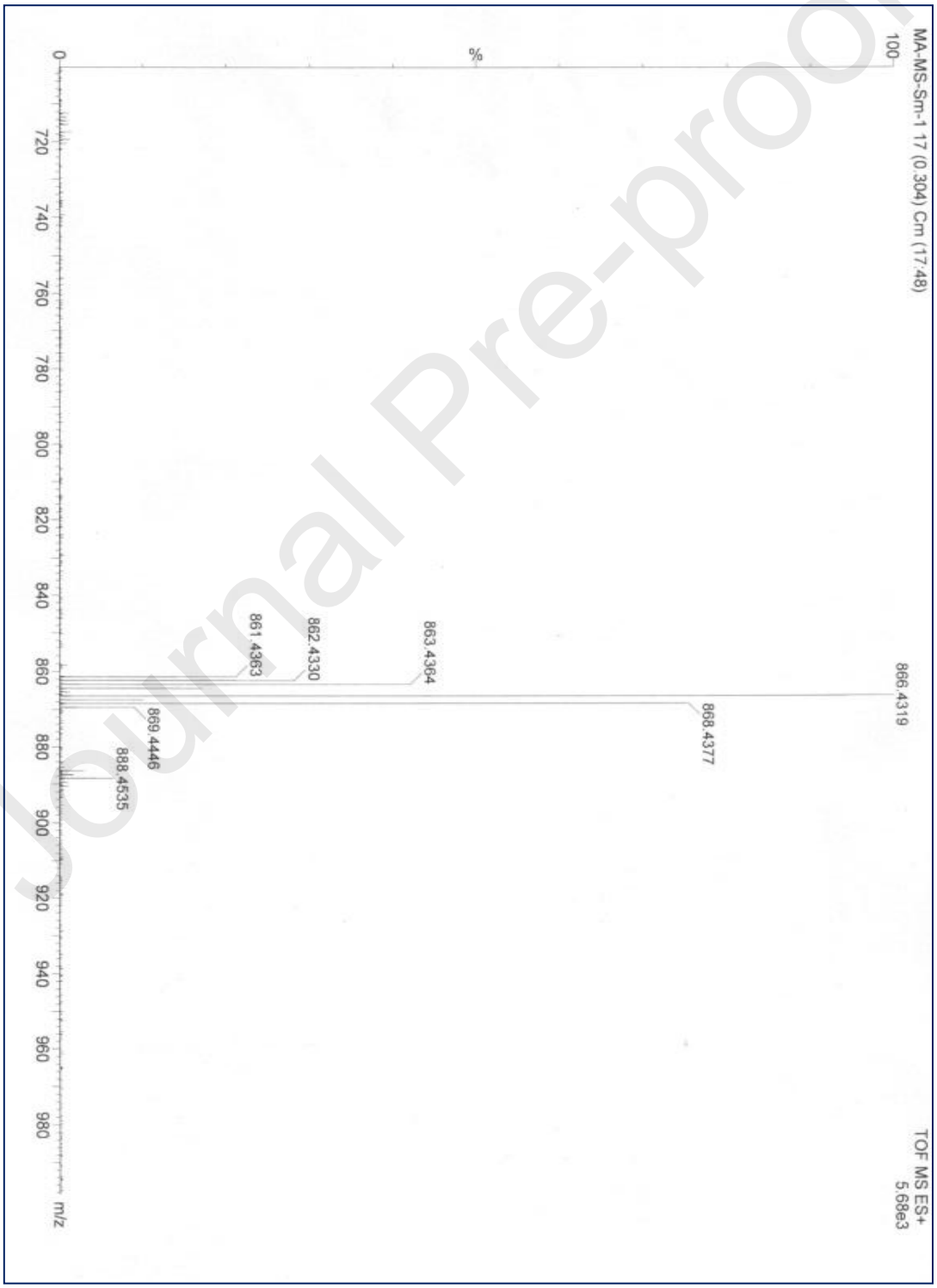

Figure S2. ESI-MS Spectra of **2**.

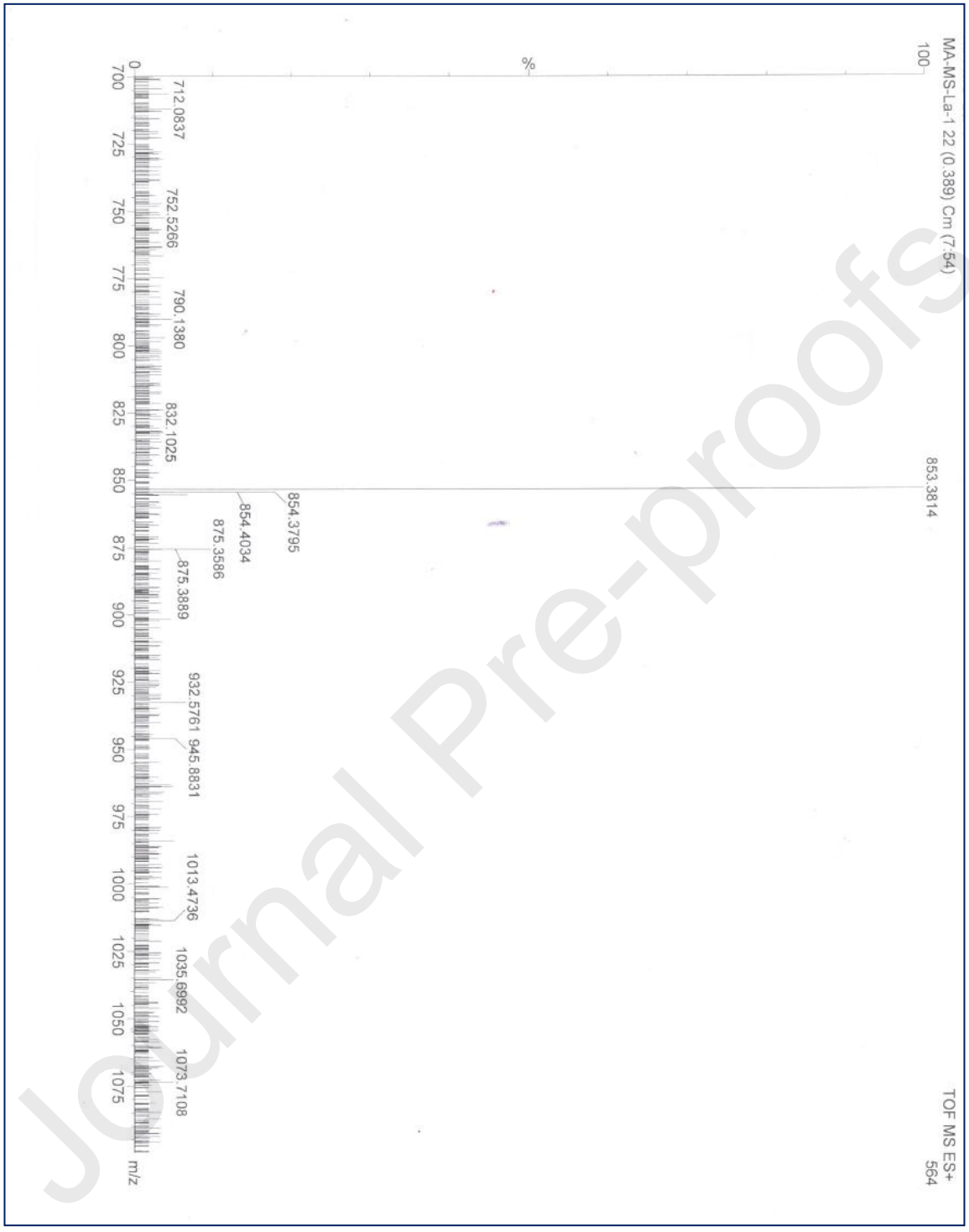

Figure S3. ESI-MS Spectra of **3**.

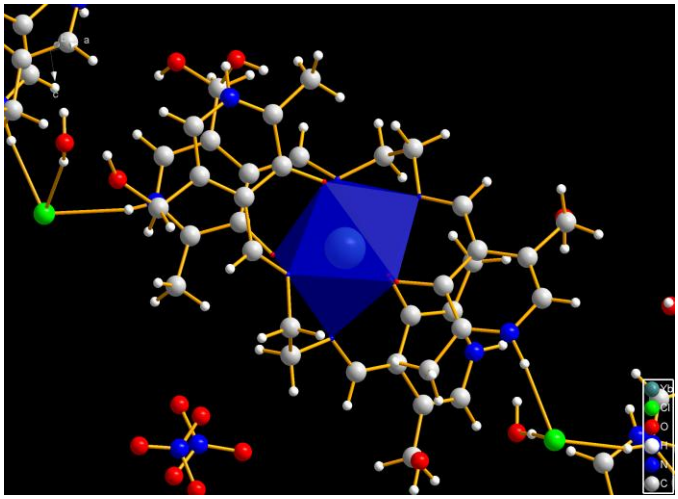

Figure S4. Coordination polyhedron of **1**.

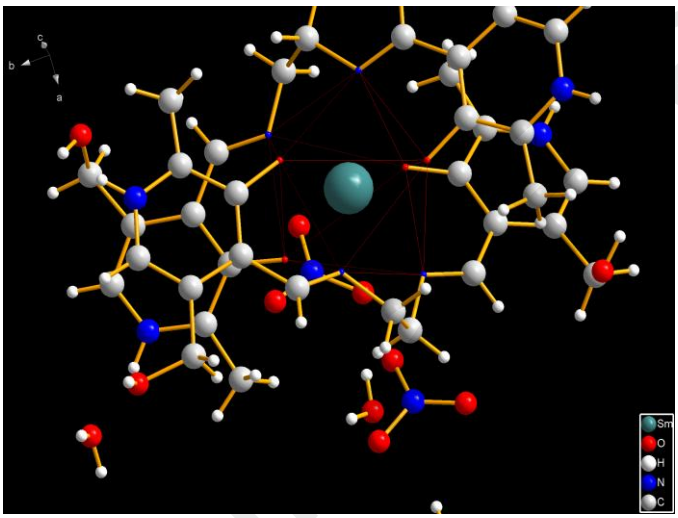

Figure S5. Coordination polyhedron of **2**.

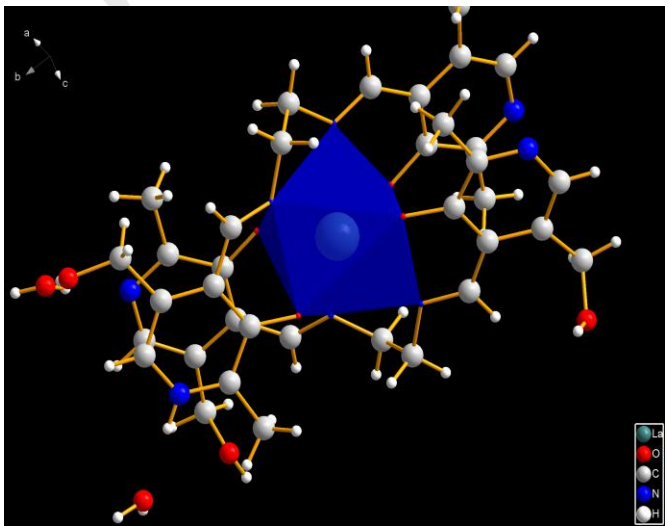

Bond angles(°)					

Figure S6. Coordination polyhedron of **2**.

Table S1. Selected bond angles in complexes **1**, **2** and **3**.

1		2		3	
O1-Yb1-O4	145.76(12)	O1-Sm1-O2	152.62(6)	O2-La1-O17	160.52(12)
O1-Yb1-O5	94.82(12)	O1-Sm1-O6	100.67(7)	O2-La1-O28	95.01(13)
O1-Yb1-O8	97.92(13)	O1-Sm1-O7	91.20(7)	O2-La1-O46	86.83(13)
O4-Yb1-O5	95.67(13)	O2-Sm1-O6	88.14(7)	O17-La1-O28	87.59(13)
O4-Yb1-O8	91.11(13)	O2-Sm1-O7	92.62(7)	O17-La1-O46	97.32(13)
O5-Yb1-O8	146.29(12)	O6-Sm1-O7	152.42(6)	O28-La1-O46	159.91(13)
N2-Yb1-N3	69.75(13)	N1-Sm1-N2	67.69(7)	N10-La1-N13	64.66(14)
N2-Yb1-N6	128.66(13)	N1-Sm1-N5	130.59(7)	N10-La1-N39	138.58(15)
N2-Yb1-N7	133.74(13)	N1-Sm1-N6	137.23(7)	N10-La1-N42	133.86(13)
N3-Yb1-N6	134.03(14)	N2-Sm1-N5	135.11(7)	N13-La1-N39	128.62(14)
N3-Yb1-N7	133.06(13)	N2-Sm1-N6	132.29(7)	N13-La1-N42	141.37(15)
N6-Yb1-N7	69.51(13)	N5-Sm1-N6	67.20(7)	N39-La1-N42	64.87(14)
O1-Yb1-N2	71.33(12)	O1-Sm1-N1	69.11(7)	O2-La1-N10	67.13(13)
O1-Yb-N3	141.06(12)	O1-Sm1-N2	136.77(7)	O2-La1-N13	131.48(13)
O1-Yb-N6	74.19(13)	O1-Sm1-N5	75.14(7)	O2-La1-N39	86.15(13)
O1-Yb-N7	76.32(12)	O1-Sm1-N6	83.03(7)	O2-La1-N42	79.67(13)
O4-Yb-N2	142.91(12)	O2-Sm1-N1	138.10(7)	O17-La1-N10	132.32(13)
O4-Yb-N3	73.18(12)	O2-Sm1-N2	70.44(7)	O17-La1-N13	67.78(13)
O4-Yb-N6	78.39(13)	O2-Sm1-N5	80.51(7)	O17-La1-N39	76.94(13)
O4-Yb-N7	75.11(13)	O2-Sm1-N6	75.54(7)	O17-La1-N42	84.39(13)
O5-Yb-N2	74.58(13)	O6-Sm1-N1	83.21(7)	O28-La1-N10	82.97(13)
O5-Yb-N3	75.99(12)	O6-Sm1-N2	75.91(7)	O28-La1-N13	74.32(14)
O5-Yb-N6	71.69(12)	O6-Sm1-N5	137.65(7)	O28-La1-N39	67.90(13)
O5-Yb-N7	141.16(13)	O6-Sm1-N6	70.47(7)	O28-La1-N42	132.70(13)
O8-Yb-N2	80.19(13)	O7-Sm1-N1	77.90(7)	O46-La1-N10	79.34(14)
O8-Yb-N3	74.51(13)	O7-Sm1-N2	78.40(6)	O46-La1-N13	89.47(13)
O8-Yb-N6	141.92(12)	O7-Sm1-N5	69.34(6)	O46-La1-N39	132.18(13)
O8-Yb-N7	72.43(13)	O7-Sm1-N6	136.23(7)	O46-La1-N42	67.33(13)

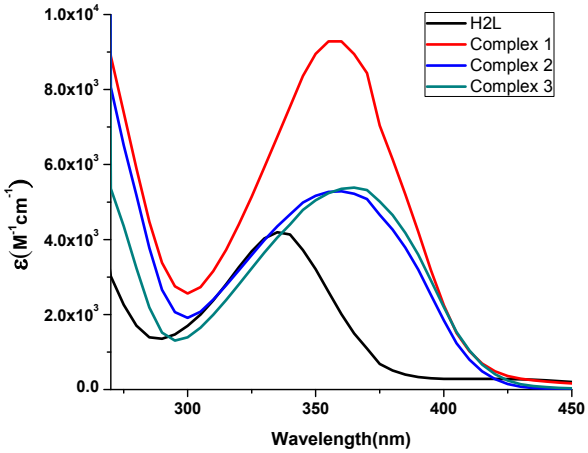

Figure S7. Electronic spectra of the ligand and the complexes in Tris-HCl buffer (pH 7.4).

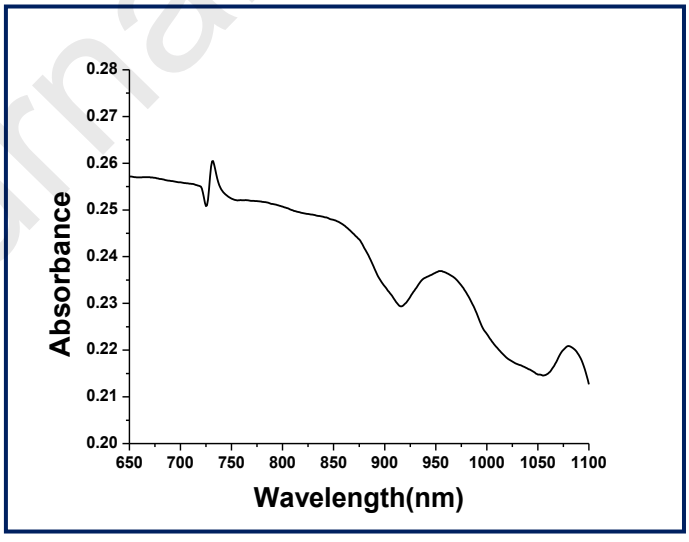

Figure S8. f-f band of **2** in NIR region.

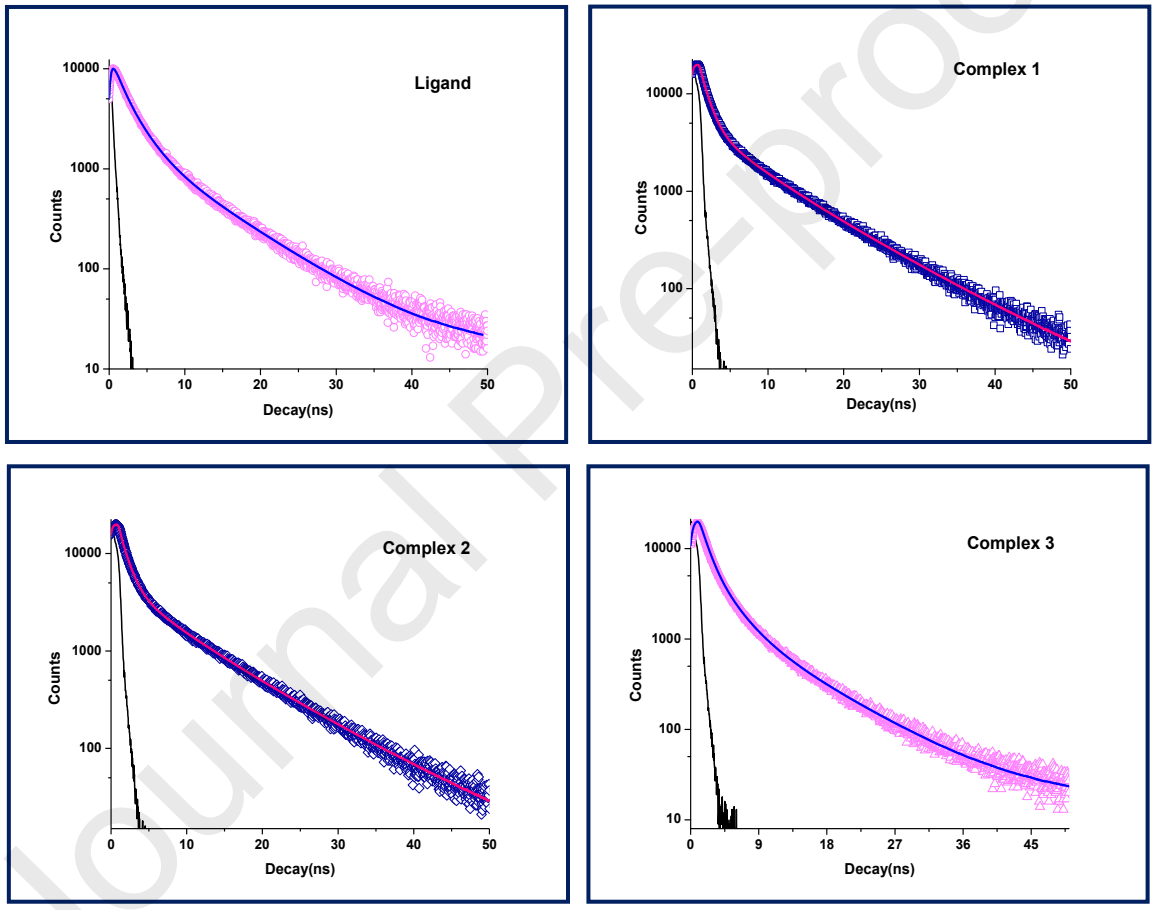

Figure S9. Time-Correlated Single Photon Counting (TCSPC) plot of the Ligand and complexes (**1**-**3**).

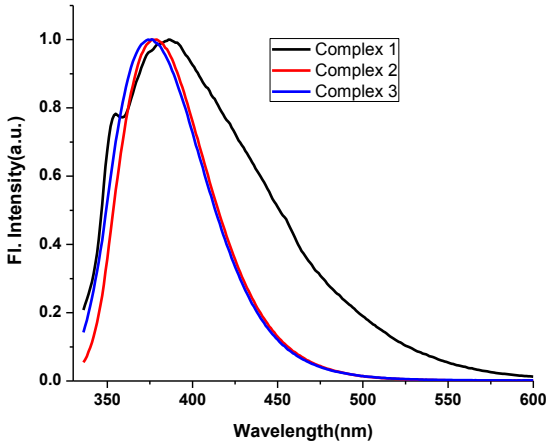

Figure S10. Ligand centred emission spectra (normalized) of the complexes in Tris-HCl buffer (pH 7.4).

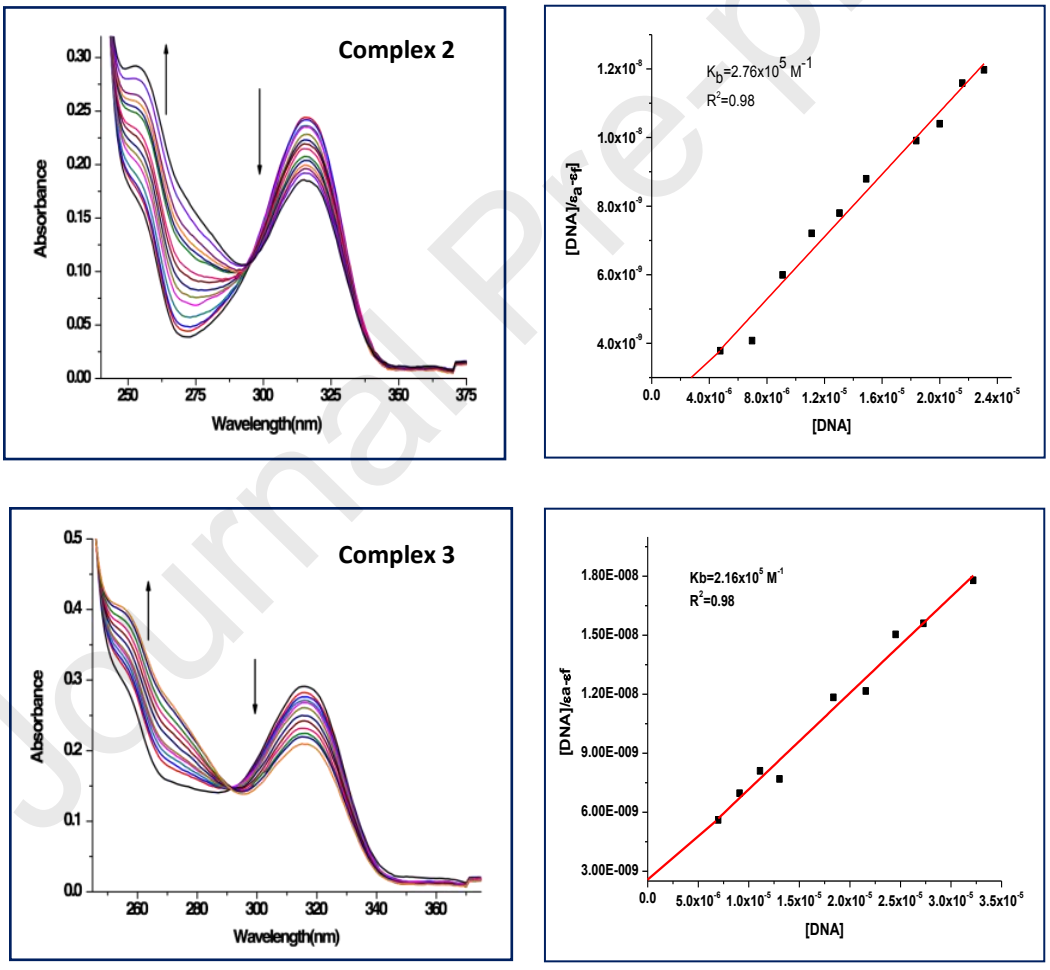

Figure S11. Absorption spectra of **2** and **3** in the absence and presence of increasing amount of CT-DNA at 25 ºC in 0.01M aqueous Tris–HCl buffer at pH 7.4 and the respective plot of [DNA]/(ε_a-ε_f) vs. [DNA].

Table S2: The average lifetime values of 1, 2 and 3 over a range of 0-7h in aqueous Tris-HCl buffer (pH 7.4) medium.

	Average Lifetime (sec)		
	0h	2h	7h
Complex 1	5.95×10^{-10}	6.39×10^{-10}	5.7×10^{-10}
Complex 2	5.52×10^{-10}	6.15×10^{-10}	5.35×10^{-10}
Complex 3	5.63×10^{-10}	6.43×10^{-10}	6.59×10^{-10}

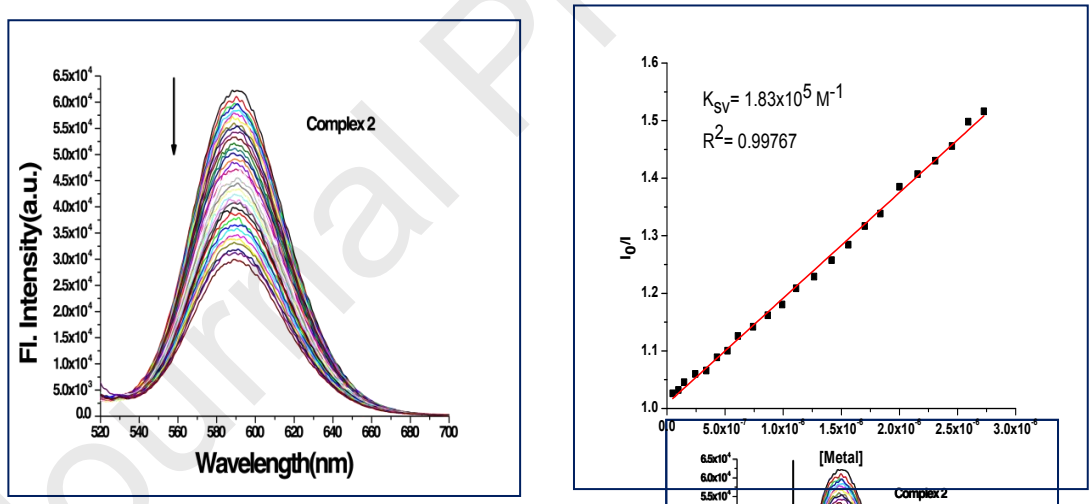

(A)

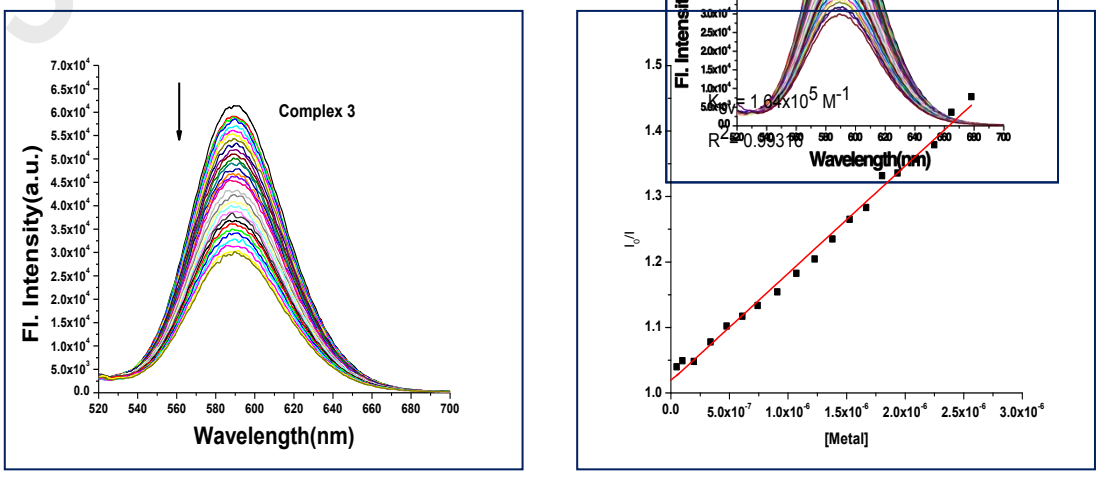

(B)

Figure S12. Emission spectra of EB bound DNA with increasing amounts of **2**(A) and **3**(B) with their respective plot of I_0/I vs. [Ln(III) complex].

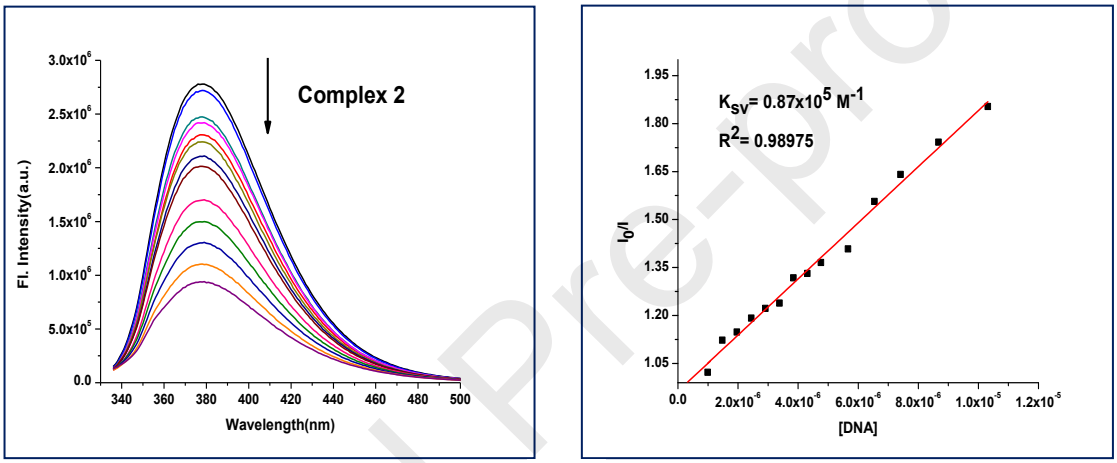

A

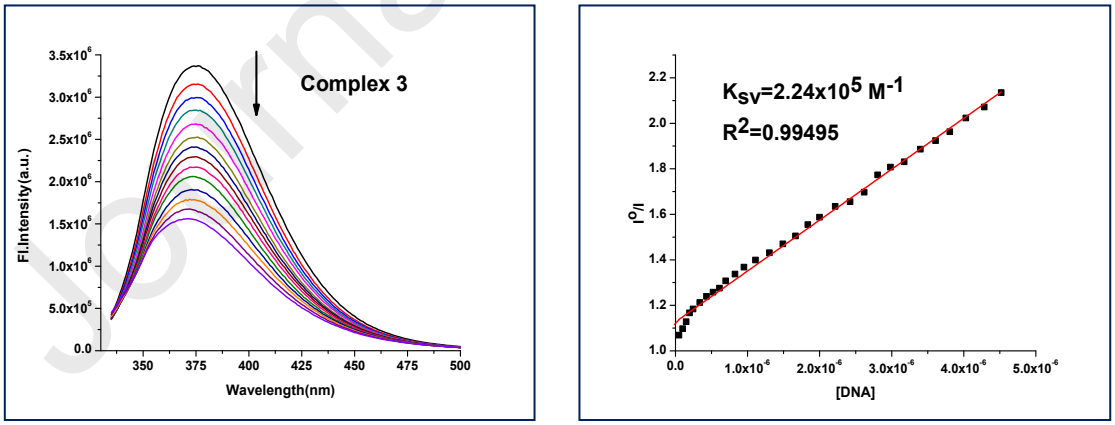

B

Figure S13. Emission spectra of **2**(A) and **3**(B) with increasing amounts of ct-DNA solution at 315nm with their respective I_0/I vs. [DNA] plot.

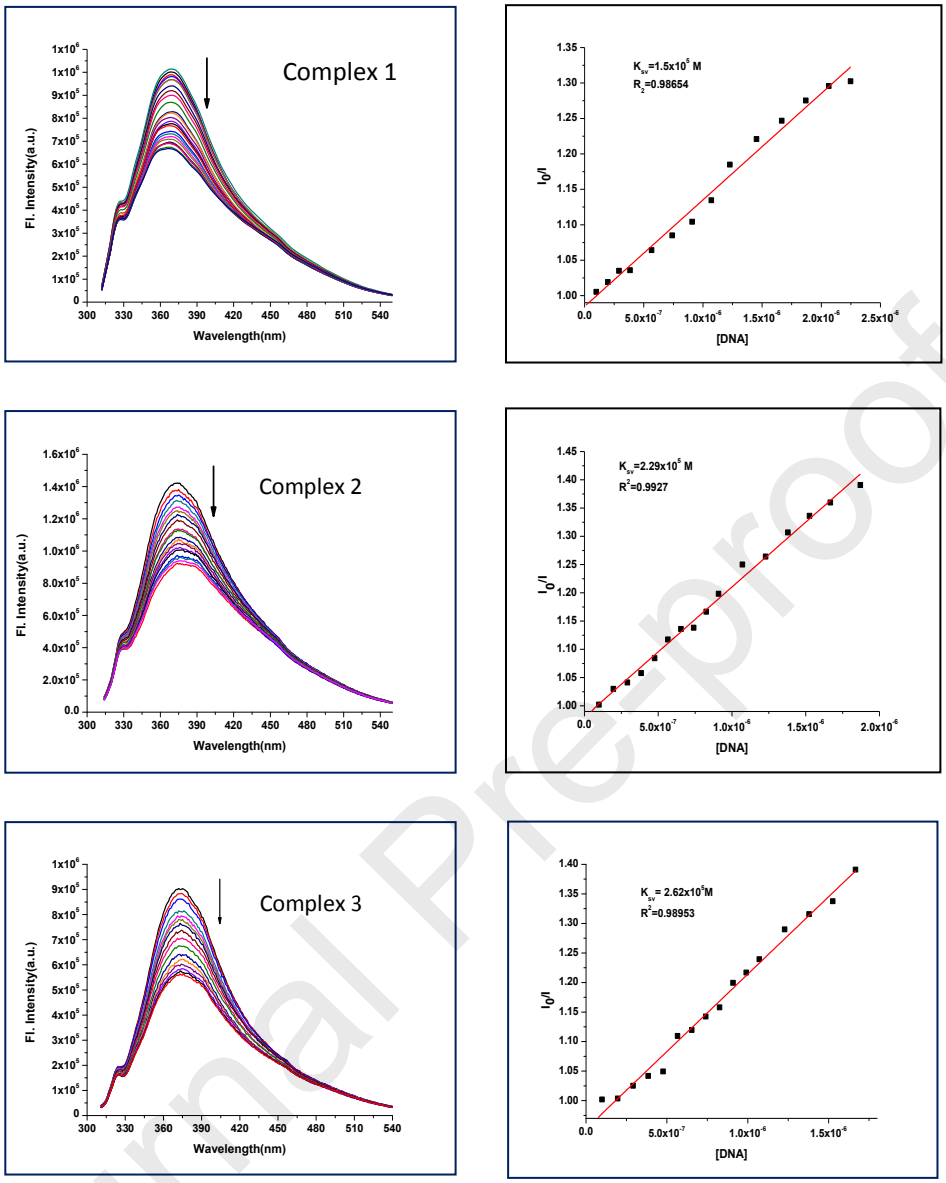

Figure S14.Emission spectra of **1, 2** and **3** with increasing amounts of ct-DNA solution at isosbestic point (Complex 1- 292nm, Complex 2- 294nm and Complex 3- 291nm) with their respective I_0/I vs. [DNA] plot.

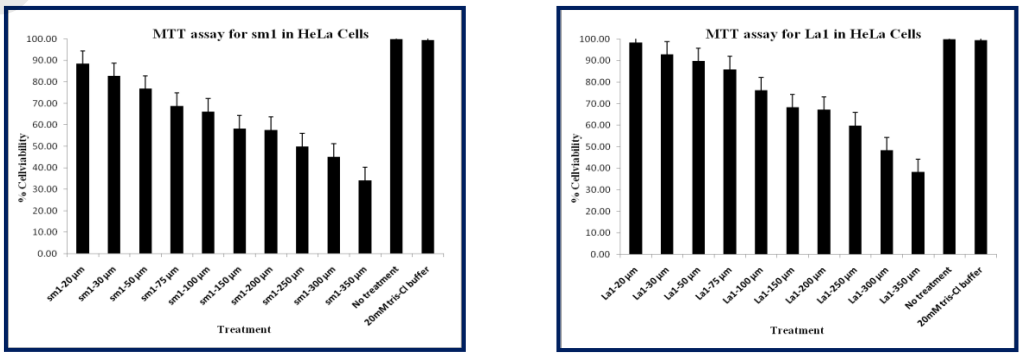

Figure S15. Cytotoxicity study of **2** and **3** on HeLa cells.

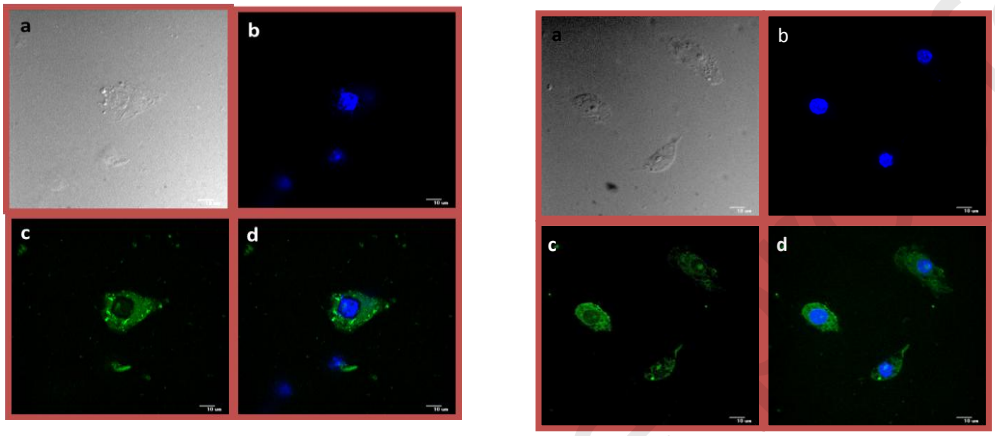

Figure S16. Confocal microscopic images of HeLa cells; all images were acquired with a 100 X objective lens. (a) Bright field image of cells (b) fluorescence images of cells without probe (**2** and **3** respectively), nuclei counterstained with Hoechst 33342 fluorescent stain (1 mg/mL) (c) fluorescence images of cells with probe (**2** and **3**), excited at 405 nm (d) overlay image of (b) and (c).